


 Cite this: *Chem. Commun.*, 2025, 61, 9420

 Received 30th April 2025,  
 Accepted 21st May 2025

DOI: 10.1039/d5cc02428e

rsc.li/chemcomm

# Unexpected cyclization of $\beta$ -(hydroxymethyl)-phosphole into 1-phospha-1,6a-dihydrophosphapentalene: a fused 1,3-butadiene-based luminophore†

 Tomohiro Higashino,<sup>id</sup>\*<sup>a</sup> Riku Minobe,<sup>a</sup> Tomoya Machino<sup>a</sup> and Hiroshi Imahori<sup>id</sup>\*<sup>abc</sup>

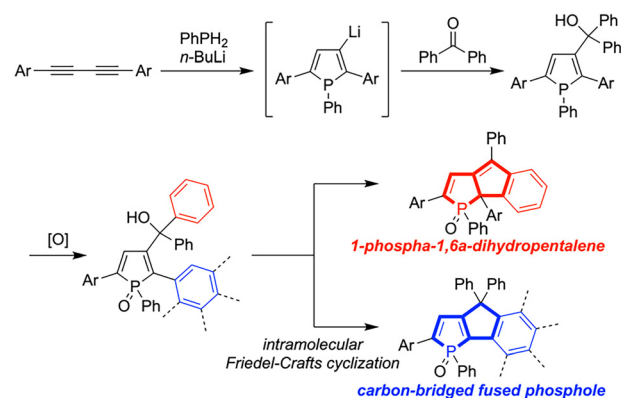
During the planned synthesis of carbon-bridged fused phospholes, an unexpected intramolecular cyclization of  $\beta$ -(hydroxymethyl)-phosphole yielded 1-phospha-1,6a-dihydropentalene, besides the expected cyclized product. The solid-state emission of 1-phospha-1,6a-dihydropentalene indicates its potential as a 1,3-butadiene-based solid-state luminophore.

Incorporating bridging structures into  $\pi$ -systems can modulate their optical and electronic properties by introducing structural constraints and electronic perturbations *via* heteroatoms. Phosphorus-bridged  $\pi$ -conjugated molecules, especially fused phosphole derivatives, exhibit remarkable physicochemical properties, such as highly electron-accepting ability and intense emission with high fluorescence quantum yields.<sup>1–9</sup> In addition, carbon-bridged structures offer optimal conjugation due to their highly planar and rigid conformation.<sup>10–15</sup> In this context, a rational synthetic methodology for carbon-bridged fused phospholes would be useful toward effectively  $\pi$ -extended phosphole-based functional materials.

Although  $\beta$ -(hydroxymethyl)phospholes serve as key precursors to carbon-bridged fused phospholes, successful synthetic protocols for  $\beta$ -substituted 2,5-diarylphospholes remain limited.<sup>16,17</sup> Given the proposed reaction mechanism for the *n*-BuLi mediated synthesis of 2,5-diarylphospholes from 1,3-butadiynes and phenylphosphine (PhPH<sub>2</sub>), we envisioned that treating 1,3-butadiynes with

a stoichiometric amount of *n*-BuLi could generate  $\beta$ -lithiated intermediates.<sup>16–18</sup> Subsequent reaction with ketones and oxidation of phosphorus atom would yield  $\beta$ -(hydroxymethyl)phosphole *P*-oxides, which could be transformed into carbon-bridged fused phosphole *P*-oxides *via* intramolecular Friedel–Crafts cyclization. Following this strategy, we pursued the straightforward synthesis of carbon-bridged fused phospholes and unexpectedly discovered the formation of 1-phospha-1,6a-dihydropentalene (Scheme 1). Though Latscha and co-workers reported the synthesis of a 1-phospha-1,6a-dihydropentalene derivative in 1991,<sup>19</sup> further exploration and detailed analysis of their properties have not been conducted. Herein, we report the intramolecular Friedel–Crafts cyclization reaction of  $\beta$ -(hydroxymethyl)phospholes, yielding 1-phospha-1,6a-dihydropentalene as well as anticipated carbon-bridged fused phospholes.

First, we embarked on synthesizing  $\beta$ -substituted 2,5-diarylphospholes (Scheme 2). Treating PhPH<sub>2</sub> with a stoichiometric amount of *n*-BuLi (1 equiv.) and subsequently adding 1,4-diphenylbutadiyne generated the  $\beta$ -lithiated phosphole intermediate at  $-78$  °C. Reacting this intermediate with benzophenone at



**Scheme 1** *n*-BuLi mediated synthesis of  $\beta$ -substituted phospholes and intramolecular Friedel–Crafts cyclization of  $\beta$ -(hydroxymethyl)phospholes.

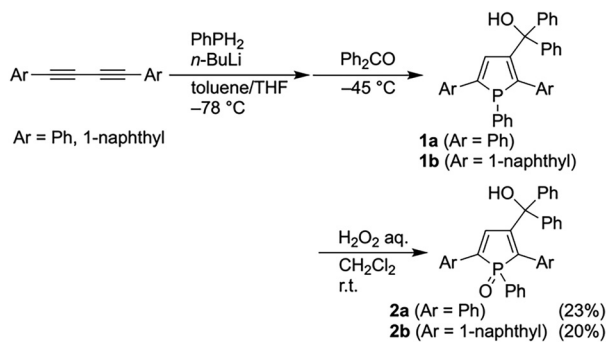
<sup>a</sup> Department of Molecular Engineering, Graduate School of Engineering, Kyoto University, Kyoto, 615-8510, Japan. E-mail: t-higa@scl.kyoto-u.ac.jp, imahori@scl.kyoto-u.ac.jp

<sup>b</sup> Institute for Integrated Cell-Material Sciences (iCeMS), Kyoto University, Kyoto, 606-8501, Japan

<sup>c</sup> Institute for Liberal Arts and Sciences (ILAS), Kyoto University, Kyoto, 606-8316, Japan

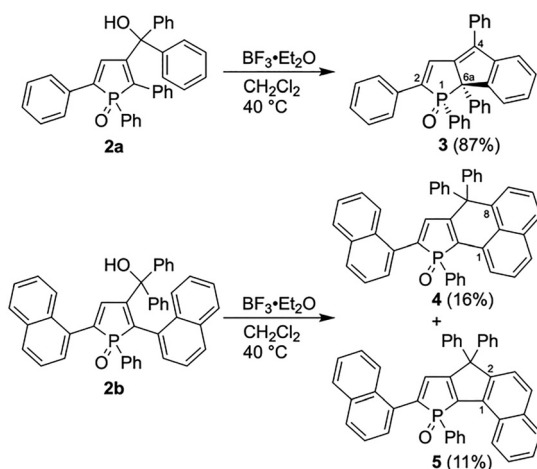
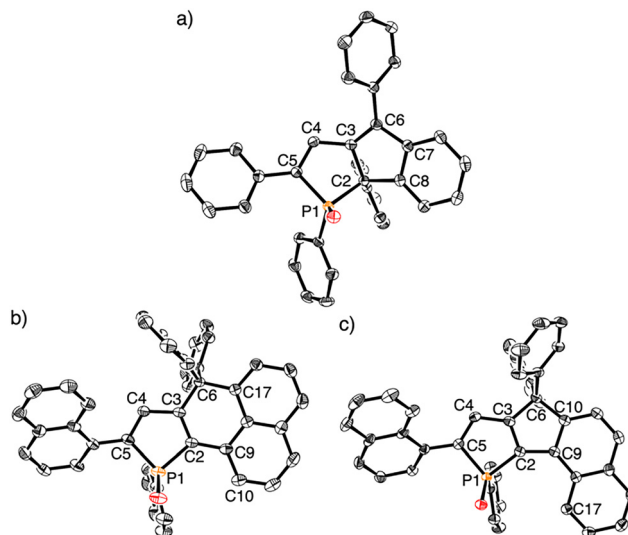
† Electronic supplementary information (ESI) available: Experimental section, synthetic details, X-ray crystallographic details, computational investigation into reaction mechanism, optical properties, HR-MS, and NMR spectra. CCDC 2424364 (3), 2424363 (4), and 2424362 (5). For ESI and crystallographic data in CIF or other electronic format see DOI: <https://doi.org/10.1039/d5cc02428e>



Scheme 2 Synthesis of  $\beta$ -(hydroxymethyl)phospholes **1** and **2**.

$-45\text{ }^{\circ}\text{C}$  then afforded the desired  $\beta$ -(hydroxymethyl)phosphole **1a**. Due to the instability of the  $\sigma^3, \lambda^3$ -phosphole **1a** under ambient conditions, it was difficult to isolate using conventional silica-gel column chromatography. Therefore, the crude **1a** was converted into the stable phosphole oxide **2a** by oxidation with an aqueous  $\text{H}_2\text{O}_2$  solution. Additionally, we synthesized the  $\beta$ -substituted phospholes **1b** and **2b** in a similar manner using 1,4-di(1-naphthyl)butadiyne.

Next, we conducted the intramolecular Friedel-Crafts cyclization reaction of phosphole *P*-oxides **2** in the presence of  $\text{BF}_3 \cdot \text{Et}_2\text{O}$  as reported by Yamaguchi and co-workers (Scheme 3).<sup>20–23</sup> When **2a** was treated with 1 equivalent of  $\text{BF}_3 \cdot \text{Et}_2\text{O}$ , it was completely recovered after conventional aqueous workup, suggesting that the stoichiometric amount of  $\text{BF}_3$  was consumed to form a phosphine oxide- $\text{BF}_3$  adduct.<sup>24,25</sup> Conversely, treating **2a** with an excess amount of  $\text{BF}_3 \cdot \text{Et}_2\text{O}$  (5 equiv.) proceeded smoothly, yielding a new product **3** in high yield (87%). Surprisingly, the crystal structure of **3** unambiguously revealed a 1-phospha-1,6a-dihydropentalene skeleton, not the anticipated carbon-bridged fused phosphole (Fig. 1a and Table S1, ESI<sup>†</sup>). Notably, the two phenyl groups at the 1- and 6a-positions adopted a *syn*-configuration, and the *anti*-isomer was not obtained. The selective formation of the *syn*-isomer can be explained by the steric hindrance of the phenyl group on the phosphorus atom in the

Scheme 3 Intramolecular cyclization reaction of phosphole *P*-oxides **2** in the presence of  $\text{BF}_3 \cdot \text{Et}_2\text{O}$ .Fig. 1 X-Ray crystal structures of (a) **3**, (b) **4**, and (c) **5**. Thermal ellipsoids represent 50% probability. Hydrogen atoms and solvent molecules are omitted for clarity.

transition state (*vide infra*). The C–C bond lengths of C2–C3 (1.5260(18) Å) and C2–C8 (1.5218(18) Å) clearly indicate that **3** possesses an  $\text{sp}^3$ -carbon atom at the 6a-position (C2 atom in Fig. 1a). The C4–C5 (1.3584(18) Å) and C3–C6 (1.3553(18) Å) bond lengths are almost comparable to a typical C=C double bond length (1.35 Å) in 1,3-butadiene.<sup>26</sup> Thus, the crystal structure clearly corroborates that **3** possesses a 1,3-butadiene skeleton.

In contrast to the reaction of **2a**, the reaction of **2b** with  $\text{BF}_3 \cdot \text{Et}_2\text{O}$  resulted in two new compounds, **4** (16%) and **5** (11%), which were successfully separated by HPLC-GPC (Scheme 3). The structures of **4** and **5** were confirmed by single crystal X-ray diffraction analysis, revealing them to be the expected carbon-bridged 1,8- and 1,2-fused phospholes, respectively (Fig. 1b, c and Table S1, ESI<sup>†</sup>). The slightly higher yield of **4** compared to **5** is attributed to the higher reactivity at the  $\alpha$ -position than the  $\beta$ -position of naphthalene.

To elucidate the reaction mechanism of the intramolecular Friedel-Crafts cyclization reactions and understand the selectivity of the products, we conducted the density functional theory (DFT) calculations at the  $\omega\text{B97XD}/6\text{-311G}++(\text{d,p})//\text{B3LYP}/6\text{-31+G}(\text{d,p})$  level with the polarizable continuum model (PCM) using  $\text{CH}_2\text{Cl}_2$  as a solvent (Tables S2 and S3, ESI<sup>†</sup>). Given that one equivalent of  $\text{BF}_3$  is consumed to form the phosphine oxide- $\text{BF}_3$  adduct (*vide supra*), we set the phosphine oxide- $\text{BF}_3$  adducts **S1** and **S2** as starting materials for the intramolecular cyclization.

First, we examined the reaction mechanism for 2,5-diphenylphosphole **S1** (Fig. 2). The hydroxy group of **S1** is activated by additional  $\text{BF}_3$ , generating the cation intermediate **INT1** via **TS1**. Intramolecular C–C bond formation then occurs via **TS2a–c**, and the deprotonation of the resultant intermediates **INT2a–c** affords the products. The energy barrier for **TS2a** ( $\Delta G^\ddagger = +17.9\text{ kcal mol}^{-1}$ ) to produce a 1-phospha-1,6a-dihydropentalene with *syn*-configuration **P1a** is smaller than those for **TS2b** ( $\Delta G^\ddagger = +20.2\text{ kcal mol}^{-1}$ ) and **TS2c** ( $\Delta G^\ddagger = +20.6\text{ kcal mol}^{-1}$ ), which yield



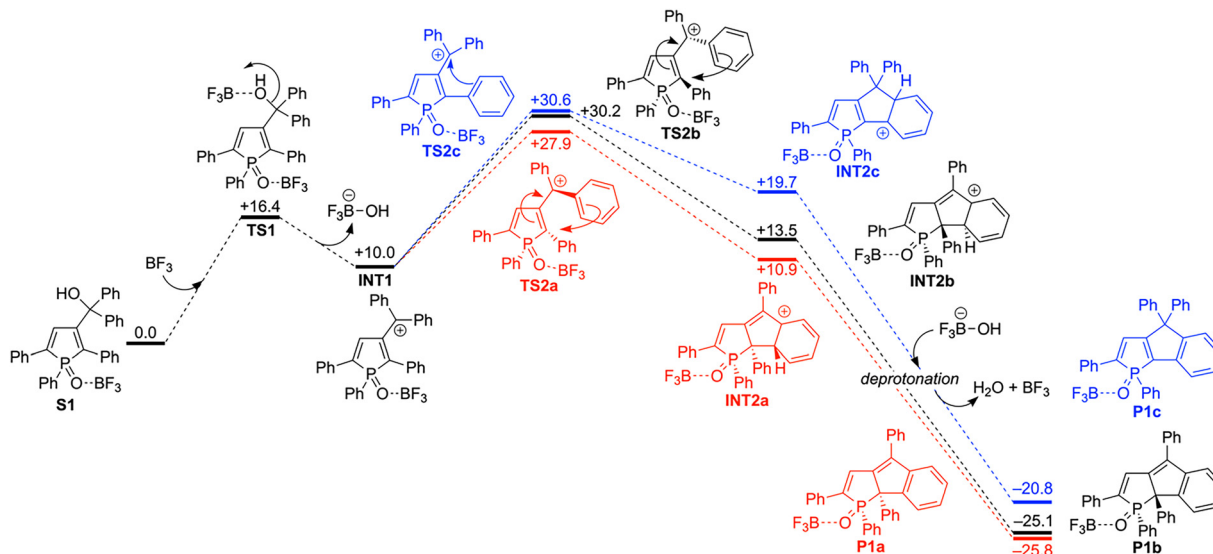


Fig. 2 Mechanistic studies of intramolecular cyclization for 2,5-diphenylphosphole **S1** using DFT methods at the  $\omega$ B97XD/6-311G++(d,p)//B3LYP/6-31+G(d,p) level with polarizable continuum model (PCM) using  $\text{CH}_2\text{Cl}_2$  as the solvent. The relative Gibbs free energy values are given in  $\text{kcal mol}^{-1}$  units.

a 1-phospha-1,6a-dihydropentalene with *anti*-configuration **P1b** and a carbon-bridged fused phosphole **P1c**, respectively. In **TS2a**, the C3–C6 bond length (1.406 Å) is significantly shorter than the non-conjugated  $\text{C}(\text{sp}^2)\text{--C}(\text{sp}^2)$  single bond length (1.48 Å),<sup>27</sup> implying the contribution of a  $\text{C}=\text{C}$  double bond (Fig. S1, ESI†). The small torsion angle of C2–C3–C6–C7 ( $19^\circ$ ) is consistent with the double bond character of the C3–C6 bond. **TS2a** thus possesses an allylic cation-like structure. Furthermore, the short H8...F1 distance in **TS2a** (2.13 Å) implies activation of the C8 atom by the  $\text{CH}\cdots\text{F}$  hydrogen bond interaction (2.20–2.26 Å).<sup>28</sup> Although the structural features of **TS2b** (C2–C3: 1.459 Å; C3–C6: 1.404 Å;  $\angle$  C2–C3–C6–C7:  $18^\circ$ ) also suggest an allylic cation-like structure, the larger torsion angle of C2–P1–O1–B1 for **TS2b** ( $73^\circ$ ) compared to **TS2a** ( $58^\circ$ ) suggests significant steric repulsion between the  $\text{BF}_3$  moiety and the phenyl ring at the 2-position, destabilizing **TS2b**.

In contrast to **TS2a** and **TS2b**, the long C3–C6 bond length (1.497 Å) and the large torsion angle of C2–C3–C6–C8 ( $81^\circ$ ) agree with the single bond character of the C3–C6 bond. As a result, the localized positive charge on the C6 atom destabilizes **TS2c**. Overall, **TS2a** is stabilized by the delocalized positive charge over the allylic cation-like structure, minimal unfavorable steric repulsion, and activation through intramolecular  $\text{CH}\cdots\text{F}$  hydrogen bond interaction. Since the C–C bond formation should be the rate-determining step, the smallest  $\Delta G^\ddagger$  value of **TS2a** clearly supports the selective formation of 1-phospha-1,6a-dihydropentalene with *syn*-configuration.

The calculated reaction mechanism for 2,5-dinaphthylphosphole **S2** is depicted in Fig. S2 (ESI†). We examined three pathways from the cation intermediate **INT3** to form the possible products, the 1-phospha-1,6a-dihydropentalene **P2a** and two carbon-bridged fused phospholes **P2b** and **P2c**. In contrast to **S1**, the  $\Delta G^\ddagger$  value of **TS4a** for forming a 1-phospha-1,6a-dihydropentalene **P2a** ( $\Delta G^\ddagger = +22.0 \text{ kcal mol}^{-1}$ ) is considerably higher than those of **TS4b** ( $\Delta G^\ddagger = +16.5 \text{ kcal mol}^{-1}$ ) and **TS4c** ( $\Delta G^\ddagger = +17.0 \text{ kcal mol}^{-1}$ ) for carbon-bridged fused phospholes **P2b** and

**P2c**. The steric hindrance of the naphthyl group at the 2-position against the diphenylmethyl group at the 3-position destabilizes **TS4a** (Fig. S3 and S4, ESI†). Moreover, the higher reactivity of the naphthyl group compared to the phenyl group toward electrophilic substitution reactions promotes the formation of carbon-bridged fused phospholes. Therefore, the selectivity of the products can be rationalized by the steric hindrance and reactivity of the aryl substituents at the 2-position on the phosphole skeleton. Additionally, the slightly smaller  $\Delta G^\ddagger$  value of **TS4b** compared to **TS4c** is attributed to the higher reactivity at the  $\alpha$ -position than the  $\beta$ -position of naphthalene, which aligns with the higher yield of 1,8-fused phosphole **4** compared to 1,2-fused phosphole **5** (*vide supra*).

We examined the optical properties of the products **3–5** (Fig. 3 and Table S4, ESI†). The blue-shifted absorption and fluorescence of **3** compared to the reference phosphole **6** can be attributed to the less effective interaction of  $\sigma^*$ -orbital of the P–C bond and  $\pi^*$ -orbital of the butadiene moiety in **3** because of the  $\text{sp}^3$  carbon atom neighboring the phosphorus atom. In addition, the *s-trans* configuration of the 1,3-butadiene skeleton in **3** may also contribute to the blue-shifted absorption.<sup>29</sup> On the other hand, the carbon-bridged fused phospholes **4** and **5** exhibit red-shifted absorption and fluorescence in comparison with the non-fused phosphole **7**. The  $\text{sp}^3$  carbon atom contributes to the effective  $\pi$ -extension resulting from the co-planarization of the naphthyl group.

Notably, 1-phospha-1,6a-dihydropentalene **3** exhibits distinct fluorescence even in the solid state whereas phosphole derivatives **4–7** show no emission in the solid state (Fig. S5, ESI†). Importantly, the  $\Phi_{\text{F}}$  value of **3** in the solid state (0.25) is considerably higher than that in solution (0.04). Given that aryl-substituted 1,3-butadiene structure have emerged as effective scaffolds for solid-state emission owing to their aggregation-induced emission (AIE) features,<sup>30–34</sup> a 1-phospha-1,6a-dihydropentalene structure can also be a promising platform for fused 1,3-butadiene-based solid-state fluorophores.



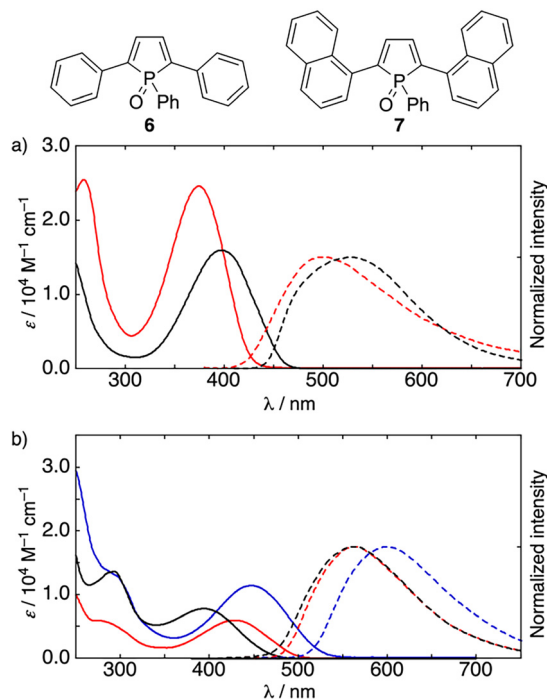


**Fig. 3** UV/Vis absorption (solid lines) and normalized fluorescence (dashed lines) spectra of (a) **3** (red) and **6** (black), and (b) **4** (red), **5** (blue), and **7** (black) in  $\text{CH}_2\text{Cl}_2$ . For fluorescence measurements, the samples were excited at  $\lambda_{\text{ex}} = 370$  nm for **3**,  $\lambda_{\text{ex}} = 430$  nm for **4**,  $\lambda_{\text{ex}} = 450$  nm for **5**, and  $\lambda_{\text{ex}} = 395$  nm for **6** and **7**.

In summary, we pursued a rational synthetic protocol for carbon-bridged fused phospholes and unexpectedly discovered an intramolecular cyclization reaction of  $\beta$ -(hydroxymethyl)-phosphole **2a**, resulting in the formation of 1-phospha-1,6a-dihydropentalene **3**. Theoretical investigations into the reaction mechanism described plausible pathways, suggesting that the product selectivity is governed by the substituents at the 2-position on the phosphole skeleton. Importantly, we revealed the solid-state emissive nature of **3** for the first time, indicating its potential as a 1,3-butadiene-based solid-state luminophore. Thus, we believe that further investigation on the intramolecular cyclization reaction of  $\beta$ -(hydroxymethyl)phospholes will pave the way for developing 1-phospha-1,6a-dihydropentalenes and carbon-bridged fused phospholes as promising organic functional materials.

This work was supported by the JSPS (KAKENHI Grant Numbers JP20H05841, JP22K05066, and JP25K01874 (T. H.), JP20H05832 and JP23H00309 (H. I.)).

## Data availability

Data supporting this article is included in the ESI.† Crystallographic data have been deposited at the CCDC with deposition numbers 2424364 (**3**), 2424363 (**4**), and 2424362 (**5**).

## Conflicts of interest

There are no conflicts to declare.

## Notes and references

- 1 Y. Matano and H. Imahori, *Org. Biomol. Chem.*, 2009, **7**, 1258–1271.
- 2 T. Baumgartner, *Acc. Chem. Res.*, 2014, **47**, 1613–1622.
- 3 D. Joly, P.-A. Bouit and M. Hissler, *J. Mater. Chem. C*, 2016, **4**, 3686–3698.
- 4 M. P. Duffy, W. Delaunay, P.-A. Bouit and M. Hissler, *Chem. Soc. Rev.*, 2016, **45**, 5296–5310.
- 5 P. Hibner-Kulicka, J. A. Joule, J. Skalik and P. Balczewski, *RSC Adv.*, 2017, **7**, 9194–9236.
- 6 N. Asok, J. R. Gaffen and T. Baumgartner, *Acc. Chem. Res.*, 2023, **56**, 536–547.
- 7 T. Higashino, K. Ishida, T. Sakurai, S. Seki, T. Konishi, K. Kamada, K. Kamada and H. Imahori, *Chem. – Eur. J.*, 2019, **25**, 6425–6438.
- 8 K. Ishida, T. Higashino, Y. Wada, H. Kaji, A. Saeki and H. Imahori, *ChemPlusChem*, 2021, **86**, 130–136.
- 9 K. Zhang, X. Wang, Z. Zhou, J. Guo, H. Liu, Y. Zhai, Y. Yao, K. Yang and Z. Zeng, *Angew. Chem., Int. Ed.*, 2025, **64**, e202418520.
- 10 U. Scherf, *J. Mater. Chem.*, 1999, **9**, 1853–1864.
- 11 H. Tsuji and E. Nakamura, *Acc. Chem. Res.*, 2019, **52**, 2939–2949.
- 12 Y. Kurumisawa, T. Higashino, S. Nimura, Y. Tsuji, H. Iiyama and H. Imahori, *J. Am. Chem. Soc.*, 2019, **141**, 9910–9919.
- 13 Y. Zhang, T. Higashino, I. Nishimura and H. Imahori, *ACS Appl. Mater. Interfaces*, 2024, **16**, 67761–67770.
- 14 J. Wang and X. Zhan, *Acc. Chem. Res.*, 2021, **54**, 132–143.
- 15 K. Wang, S. Jinnai, T. Urakami, H. Sato, M. Higashi, S. Tsujimura, Y. Kobori, R. Adachi, A. Yamakata and Y. Ie, *Angew. Chem., Int. Ed.*, 2024, **63**, e202412691.
- 16 D. Klintuch, K. Krekić, C. Bruhn, Z. Benkó and R. Pietschnig, *Eur. J. Inorg. Chem.*, 2016, 718–725.
- 17 F. Roesler, M. Kovács, C. Bruhn, Z. Kelemen and R. Pietschnig, *Organometallics*, 2023, **42**, 793–802.
- 18 G. Märkl and R. Potthast, *Angew. Chem., Int. Ed. Engl.*, 1967, **6**, 86.
- 19 J. Silberzahn, H. Pritzkow and H. P. Latscha, *Z. Naturforsch. B*, 1991, **46**, 197–201.
- 20 A. Fukazawa, Y. Ichihashi, Y. Kosaka and S. Yamaguchi, *Chem. – Asian J.*, 2009, **4**, 1729–1740.
- 21 C. Wang, A. Fukazawa, M. Taki, Y. Sato, T. Higashiyama and S. Yamaguchi, *Angew. Chem., Int. Ed.*, 2015, **54**, 15213–15217.
- 22 R. A. Adler, C. Wang, A. Fukazawa and S. Yamaguchi, *Inorg. Chem.*, 2017, **56**, 8718–8725.
- 23 C. Wang, M. Taki, Y. Sato, A. Fukazawa, T. Higashiyama and S. Yamaguchi, *J. Am. Chem. Soc.*, 2017, **139**, 10374–10381.
- 24 N. Burford, R. E. V. H. Spence, A. Linden and T. S. Cameron, *Acta Crystallogr., Sect. C: Cryst. Struct. Commun.*, 1990, **46**, 92–95.
- 25 V. M.-Y. Leung, H.-C. F. Wong, C.-M. Pook, Y.-L. S. Tse and Y.-Y. Yeung, *Chem. Sci.*, 2023, **14**, 12684–12692.
- 26 F. H. Allen, O. Kennard, D. G. Watson, L. Brammer, A. G. Orpen and R. Taylor, *J. Chem. Soc., Perkin Trans. 2*, 1987, S1–S19.
- 27 K. Kveseth, R. Seip and D. A. Kohl, *Acta Chem. Scand.*, 1980, **34a**, 31–42.
- 28 E. Kryachko and S. Scheiner, *J. Phys. Chem. A*, 2004, **108**, 2527–2535.
- 29 M. E. Squillacote, R. S. Sheridan, O. L. Chapman and F. A. L. Anet, *J. Am. Chem. Soc.*, 1979, **101**, 3657–3659.
- 30 M. K. Bera, C. Chakraborty and S. Malik, *J. Mater. Chem. C*, 2017, **5**, 6872–6879.
- 31 Y. Zhang, H. Mao, W. Xu, J. Shi, Z. Cai, B. Tong and Y. Dong, *Chem. Eur. J.*, 2018, **24**, 15965–15977.
- 32 M. K. Bera, P. Pal and S. Malik, *J. Mater. Chem. C*, 2020, **8**, 788–802.
- 33 P. Pal, A. Datta, S. Mukherjee, A. Perumal and S. Malik, *J. Mater. Chem. C*, 2023, **11**, 16594–16604.
- 34 P. Pal, A. Datta, R. Mondal and S. Malik, *ACS Appl. Polym. Mater.*, 2024, **6**, 6001–6009.

